

Crystal Structures and Molecular Packing of Tetrakis(alkylthio)tetrathiafulvalene (TTC_n-TTF); (Part II) (*n*=7,9,11)

Chikako NAKANO,^{*,†††} Takehiko MORI, Kenichi IMAEDA, Noritake YASUOKA,[†]
Yusei MARUYAMA, Hiroo INOKUCHI, Naoko IWASAWA,^{††}
and Gunzi SAITO^{†††}

Institute for Molecular Science, Myodaiji, Okazaki 444

[†]Basic Research Laboratory, Himeji Institute of Technology, Shosha, Himeji 671-22

^{††}The Institute for Solid State Physics, The University of Tokyo, Roppongi, Minato-ku, Tokyo 106

^{†††}Department of Chemistry, Faculty of Science, Kyoto University, Sakyo-ku, Kyoto 606

(Received December 5, 1991)

The crystal structures of tetrakis(alkylthio)tetrathiafulvalene (TTC_{*n*}-TTF) with long alkyl chains ($7 \leq n \leq 11$) can be divided into two different groups (Form I and Form II) according to the difference in the arrangement of the alkyl chains. Although the crystals of TTC₇-TTF exhibit two phases (triclinic and monoclinic), the stacking manner of these phases is nearly the same, Form II. TTC₉-TTF crystallizes in two different forms: Form I (the triclinic phase) and Form II (the monoclinic phase). The TTC₁₁-TTF crystal only adopts the Form I structure. Although the molecules in both forms have chair-like shapes and columnar structures, the alkyl chains in the Form I crystals are arranged parallel to each other, resulting in more strongly fastened packing than in the case of the Form II crystals. These results are associated with changes in the electrical resistivities and activation energies of TTC_{*n*}-TTF over the range of large *n*.

A previous paper¹⁾ (Part I) reported the crystal structures of the short alkyl chain members of TTC_{*n*}-TTF and discussed the differences in the structures as well as some properties between *n*=3 and 4. The long-chain systems were found to show lower resistivities than those of the short-chain systems (ca. 10² Ω cm). In addition, those compounds with large *n* (*n*≥8) revealed solid–solid phase transitions in DSC measurements;²⁾

especially, TTC₈-TTF has revealed transitions in the electrical conductivity³⁾ and mobility.⁴⁾ The long alkyl chains in TTC_{*n*}-TTF must therefore play an important role in changes of their solid state properties at around *n*=8. In this paper we report on the crystal structures of long alkyl chain systems (*n*=7, 9, 11), and discuss the characteristic electrical resistivities of TTC_{*n*}-TTF⁵⁾ in terms of the difference in the crystal molecular packings.

Table 1. Crystal Data

	TTC ₇ -TTF C ₃₄ H ₆₀ S ₈	TTC ₉ -TTF C ₄₂ H ₇₆ S ₈	TTC ₁₁ -TTF C ₅₀ H ₉₂ S ₈
F.W.	725.37	837.58	949.80
Crystal size/mm ³	(0.1×0.05×0.3)	(0.25×0.03×0.6)	(0.2×0.1×0.4)
Space group	<i>P</i> 2 ₁ / <i>a</i>	<i>P</i> $\bar{1}$	<i>P</i> $\bar{1}$
<i>a</i> /Å	8.797(2)	8.802(3)	7.857(1)
<i>b</i> /Å	46.90(1)	23.479(4)	30.518(2)
<i>c</i> /Å	5.141(1)	5.152(2)	5.119(1)
α /°	90.0	90.66(2)	92.81(2)
β /°	103.89(2)	103.72(3)	101.40(1)
γ /°	90.0	95.33(3)	85.77(1)
<i>V</i> /Å ³	2059.2(9)	1029(8)	1199(2)
<i>Z</i>	2	1	1
<i>d</i> _{calcd} /g cm ⁻³	1.170	1.171	1.160
X-Ray	Mo <i>K</i> α	Cu <i>K</i> α	Cu <i>K</i> α
μ(X-ray)/cm ⁻¹	4.371	41.12	35.86
Scan mode	θ–2θ	ω–2θ	ω–2θ
2θ _{max} /°	60	120	120
Diffractometer	Rigaku AFC-5	Enraf-Nonius CAD4	Enraf-Nonius CAD4
Reflections measured	2343	3444	3966
Reflections used ($ F_o > 3\sigma(F_o)$)	657	2675	3186
<i>R</i>	0.092	0.055	0.054
<i>wR</i>	0.115	0.072	0.072
(Δ/ <i>σ</i>) _{max}	0.49	0.84	0.84
Residual density/e Å ⁻³	0.6 to –0.4	0.4 to –0.3	0.8 to –0.5

^{†††} Toyota research fellow.

Experimental

The syntheses of $\text{TTC}_n\text{-TTF}$ compounds were reported in previous papers.^{6,7)} Single crystals were prepared by recrystallization from mixed solvents of hexane and ethanol. Two different kinds of $\text{TTC}_7\text{-TTF}$ crystals were grown as orange needle crystals; it is difficult to distinguish between these two species visually. Although the triclinic phase was mainly obtained, the monoclinic phase tends to be obtained from a saturated solution at room temperature. Two different types of $\text{TTC}_9\text{-TTF}$ crystals were obtained: orange needle-like crystals (monoclinic phase) were from a solution at room temperature,⁵⁾ while orange plate-like crystals (the triclinic phase) were from a solution at below room temperature. The $\text{TTC}_{11}\text{-TTF}$ crystals were grown as orange plate crystals. It was very difficult to obtain single crystals of compounds with $n \geq 12$. Crystal data are shown in Table 1. For all of the crystals, the intensity variation of standard reflections were less than 5%. The number of reflections of $\text{TTC}_7\text{-TTF}$ (the monoclinic phase) is much less than those of the other crystals, since the used single crystal was very thin. The structures were solved by the Patterson method (for $n=7$ and 11) as well as by a direct method using the MULTAN 82 program system⁸⁾ (for $n=9$). The atomic parameters were refined by a block-diagonal least squares procedure $\{w=[\sigma(F_o)^2+(0.015 F_o)^2]^{-1}\}$ after an absorption correction (Gaussian Integration procedure). The reason for the high R value of $\text{TTC}_7\text{-TTF}$ (the monoclinic phase) and $\text{TTC}_{11}\text{-TTF}$ could be the poor quality of the crystals. The positions of the H atoms of $\text{TTC}_7\text{-TTF}$ (the triclinic phase) and $\text{TTC}_9\text{-TTF}$ were found from difference Fourier maps; those of the other crystals were calculated. Anisotropic temperature factors were used for refining the non-hydrogen atoms and isotropic temperature factors were adopted for the hydrogen atoms. The atomic scattering factors were taken from the International Tables for X-Ray Crystallography.⁹⁾ The calculations were carried out on a HITAC M-680H computer with the UNICS III program system¹⁰⁾ as well as a MicroVAX II computer with the SDP software package.¹¹⁾

Results

$\text{TTC}_7\text{-TTF}$ (the Triclinic Phase): The molecular structure is shown in Fig. 1(a) and final atomic coordinates and thermal temperature factors are shown in Table 2.¹²⁾ The crystal structure is isostructural to that of $\text{TTC}_8\text{-TTF}$ (Form II).³⁾ The molecule has a chair-like shape and is centrosymmetric. The four heptyl chains are far from perpendicular to the central tetrathio-TTF skeleton. One alkyl chain is slightly bent, compared with the other chain; these heptyl chains do not elongate parallel to each other (the Chair II type). The molecules are stacked face to face along the c -axis, thus making a columnar structure (Fig. 2(a)) with an overlapping mode, as shown in Fig. 3(a). The central C_6S_8 groups are planar and the distance between the two least-squares planes of the C_6S_8 groups along the stacking axis is 3.49 Å. The shortest intracolumnar S...S distance is 3.591(2) Å, which is nearly equal to that of $\text{TTC}_8\text{-TTF}$ (Form II) (3.595(4) Å).³⁾ On the other hand, there is no short intercolumnar S...S dis-

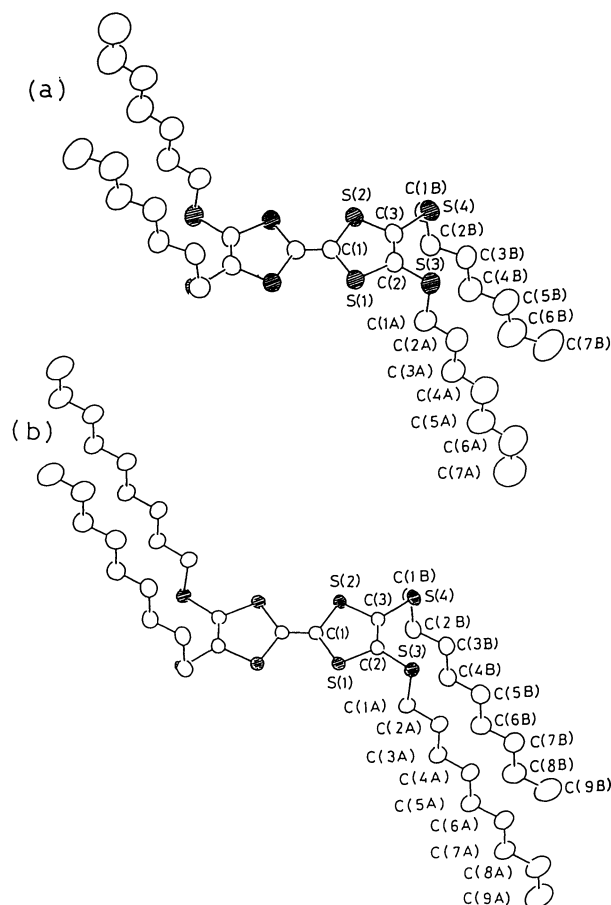


Fig. 1. Molecular structure and atomic numbering scheme (a) $\text{TTC}_7\text{-TTF}$ (the triclinic phase) [Form II (T)] (b) $\text{TTC}_9\text{-TTF}$ (the triclinic phase) [Form I].

Table 2. Fractional Atomic Coordinates ($\times 10^4$) and Equivalent Isotropic Temperature Factors of $\text{TTC}_7\text{-TTF}$ (The Triclinic Phase)

$$B_{eq} = \frac{4}{3} (\sum_i \sum_j B_{ij} a_i \cdot a_j)$$

Atom	x	y	z	$B_{eq}/\text{\AA}^2$
S(1)	5683(1)	895(0)	1368(2)	4.7
S(2)	3253(1)	36(0)	2393(2)	4.4
S(3)	4766(1)	1832(0)	4454(2)	5.9
S(4)	2018(1)	843(0)	5735(2)	5.1
C(1)	4775(4)	196(2)	761(7)	4.1
C(2)	4422(4)	1122(2)	3262(7)	4.4
C(3)	3327(4)	730(2)	3735(7)	4.3
C(1A)	4255(7)	2201(2)	1301(10)	7.9
C(2A)	4061(6)	2805(2)	1720(11)	7.7
C(3A)	3644(7)	3128(2)	-850(11)	8.5
C(4A)	3419(8)	3736(3)	-479(14)	10.0
C(5A)	3026(8)	4059(3)	-2999(13)	10.4
C(6A)	2740(10)	4667(3)	-2683(17)	13.3
C(7A)	2431(11)	4981(4)	-4987(18)	15.1
C(1B)	140(4)	727(2)	3272(9)	5.6
C(2B)	-124(4)	1179(2)	1202(8)	5.2
C(3B)	-283(5)	1770(2)	2353(9)	6.0
C(4B)	-726(6)	2193(2)	162(10)	7.2
C(5B)	-919(6)	2779(2)	1249(12)	8.6
C(6B)	-1444(8)	3199(3)	-896(16)	11.3
C(7B)	-1627(10)	3768(3)	204(20)	14.3

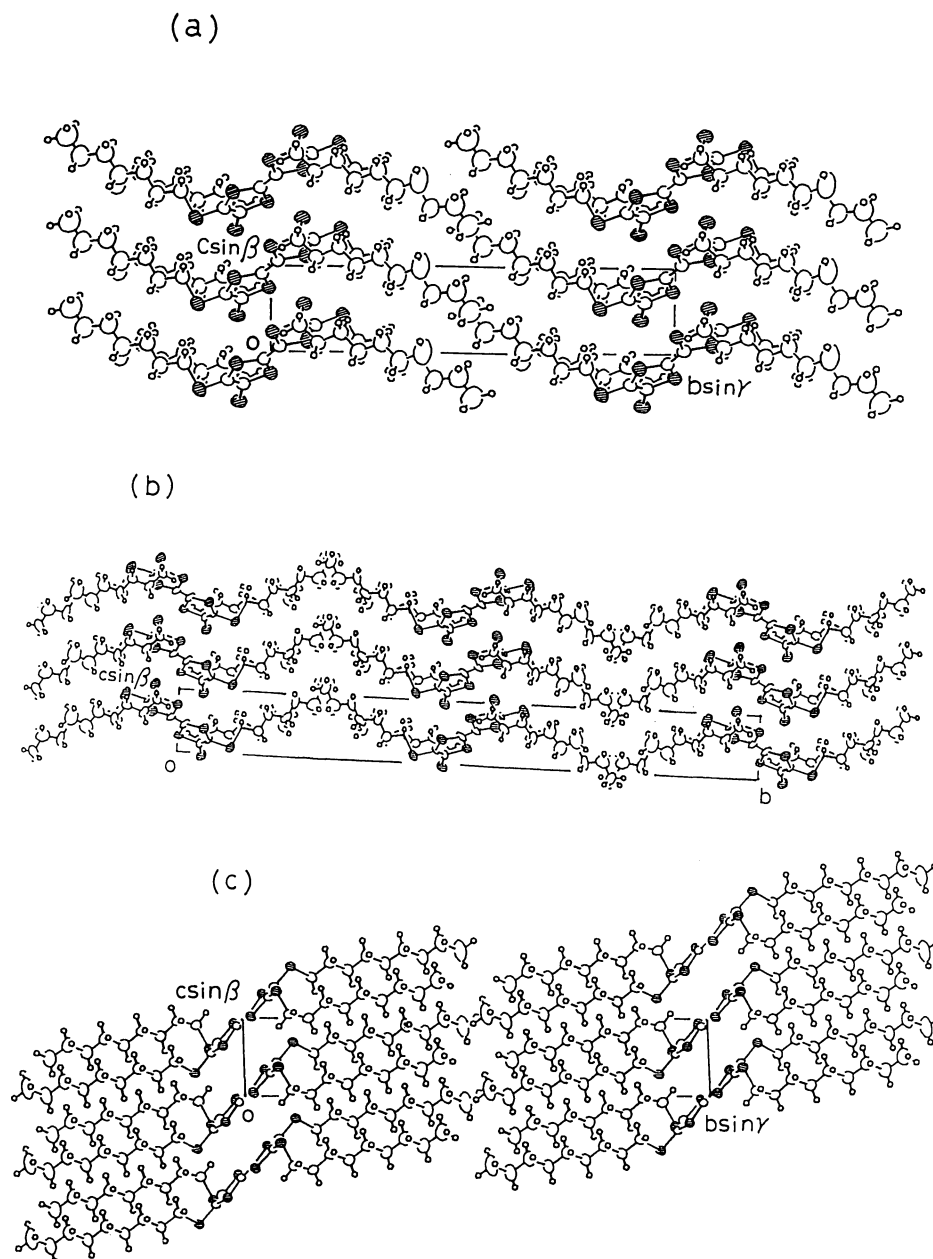


Fig. 2. Crystal structure along the a -axis (a) Forms II (T) ($n=7$ (the triclinic phase)) (b) Form II (M) ($n=7$ (the monoclinic phase)) (c) Form I ($n=9$ (the triclinic phase)).

tance ($<4 \text{ \AA}$).

TTC₇-TTF (the Monoclinic Phase): The numbering scheme is the same as that of TTC₇-TTF (the triclinic phase). The final atomic parameters are listed in Table 3.¹²⁾ The crystal structure (Fig. 2(b)) is isostructural to that of TTC₉-TTF (the monoclinic phase).⁵⁾ The molecular shape is nearly the same as the triclinic phase (Chair II). The distance between the adjacent least-squares planes of the central C₆S₈ groups along the stacking axis is 3.49 \AA , which is the same as that of the triclinic phase. Although the shortest intracolumnar S...S distance ($3.54(1) \text{ \AA}$) is shorter than that of the triclinic phase, the intermolecular overlapping seems to

be slightly less, as is shown in Fig. 3(b).

TTC₉-TTF (the Triclinic Phase): The molecular structure is shown in Fig. 1(b). The final atomic parameters are listed in Table 4.¹²⁾ The crystal structure (Fig. 2(c)) is isostructural to TTC₈-TTF (Form I)³⁾ and TTC₁₀-TTF.⁵⁾ The molecular structure is chair-like and the alkyl chains are elongated parallel to each other (Chair I type). The molecules are arranged face to face along the c -axis and the interplanar distance between the adjacent central C₆S₈ skeletons along the stacking axis is 3.46 \AA . The intermolecular overlapping mode (Fig. 3(c)) is similar to that of TTC₈-TTF (Form I), larger than those of TTC₇-TTF of the triclinic

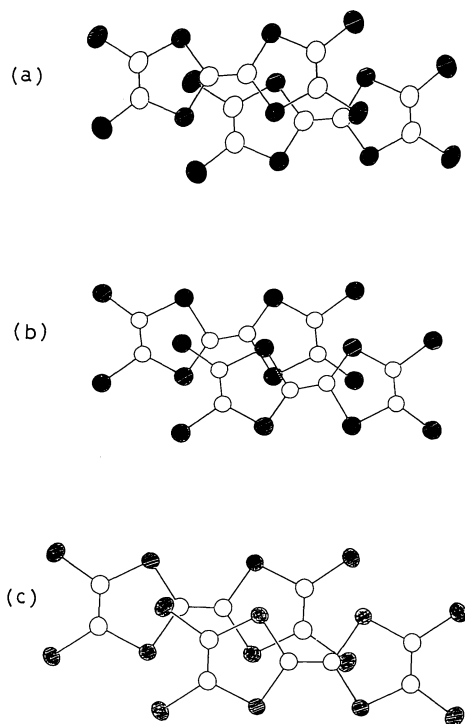


Fig. 3. Mode of overlap along the c -axis (a) Form II (T) ($n=7$ (the triclinic phase)) (b) Form II (M) ($n=7$ (the monoclinic phase)) (c) Form I ($n=9$ (the triclinic phase)).

Table 3. Fractional Atomic Coordinates ($\times 10^4$) and Equivalent Isotropic Temperature Factors of $\text{TTC}_7\text{-TTF}$ (The Monoclinic Phase)

Atom	x	y	z	$B_{\text{eq}}/\text{\AA}^2$
S(1)	1745(13)	16(2)	2580(22)	3.7
S(2)	-425(13)	449(3)	3811(23)	4.3
S(3)	3250(13)	423(3)	-537(22)	4.6
S(4)	801(14)	921(2)	934(24)	4.9
C(1)	258(49)	115(8)	4436(81)	4.5
C(2)	1957(42)	384(8)	1368(70)	3.6
C(3)	921(42)	548(7)	1948(66)	3.2
C(1A)	5126(40)	380(8)	1910(74)	3.5
C(2A)	5465(44)	601(9)	3970(78)	4.7
C(3A)	5826(49)	898(9)	2958(78)	5.0
C(4A)	6421(51)	1106(8)	5149(89)	6.0
C(5A)	6784(53)	1389(10)	4129(99)	7.5
C(6A)	7394(68)	1584(12)	6605(110)	10.9
C(7A)	7741(70)	1849(12)	5211(131)	12.7
C(1B)	1401(51)	1099(7)	4217(78)	4.6
C(2B)	1784(53)	1402(9)	3808(84)	6.1
C(3B)	2299(56)	1553(9)	6516(89)	6.7
C(4B)	2667(57)	1864(10)	6202(83)	7.0
C(5B)	3293(68)	2019(10)	8766(110)	10.1
C(6B)	3587(78)	2329(12)	8477(118)	12.3
C(7B)	4291(69)	2477(11)	11105(106)	10.7

and monoclinic phases. Furthermore, the shortest intracolumnar S...S distance (3.581(1) \AA) is slightly shorter than those of the $\text{TTC}_8\text{-TTF}$ crystals (Form I: 3.5834(9) \AA (at 0°C), Form II: 3.595(4) \AA (at room temperature)).³⁾ In addition, the molecules are

Table 4. Fractional Atomic Coordinates ($\times 10^4$) and Equivalent Isotropic Temperature Factors of $\text{TTC}_9\text{-TTF}$ (Form I)

Atom	x	y	z	$B_{\text{eq}}/\text{\AA}^2$
S(1)	703(1)	450(0)	3463(1)	2.6
S(2)	-2691(1)	181(0)	440(1)	2.8
S(3)	-872(1)	1082(0)	7082(1)	3.1
S(4)	-4747(1)	747(0)	3834(1)	3.0
C(1)	-412(4)	133(1)	800(5)	2.4
C(2)	-1174(4)	702(1)	4391(6)	2.7
C(3)	-2725(4)	577(1)	3044(6)	2.6
C(1A)	48(4)	1521(1)	5627(7)	3.8
C(2A)	55(5)	1923(1)	7509(7)	4.0
C(3A)	805(5)	2315(1)	6513(8)	4.5
C(4A)	723(5)	2718(1)	8358(8)	4.7
C(5A)	1432(6)	3121(1)	7413(9)	5.3
C(6A)	1290(6)	3525(1)	9238(9)	5.6
C(7A)	1948(6)	3934(1)	8276(10)	6.4
C(8A)	1815(8)	4335(1)	10120(13)	8.3
C(9A)	2434(10)	4740(2)	9146(16)	11.6
C(1B)	-5828(4)	1017(1)	783(6)	3.5
C(2B)	-4997(4)	1427(1)	226(6)	3.7
C(3B)	-5056(5)	1805(1)	2267(7)	4.0
C(4B)	-4312(5)	2212(1)	1490(7)	4.5
C(5B)	-4412(5)	2611(1)	3400(8)	4.8
C(6B)	-3684(5)	3016(1)	2502(8)	5.3
C(7B)	-3803(6)	3420(1)	4353(9)	5.8
C(8B)	-3081(7)	3822(1)	3426(10)	7.0
C(9B)	-3221(8)	4226(2)	5241(13)	9.0

Table 5. Fractional Atomic Coordinates ($\times 10^4$) and Equivalent Isotropic Temperature Factors of $\text{TTC}_{11}\text{-TTF}$ (Form I)

Atom	x	y	z	$B_{\text{eq}}/\text{\AA}^2$
S(1)	659(3)	386(1)	3391(6)	2.9
S(2)	-2719(4)	155(1)	421(6)	3.0
S(3)	-983(4)	931(1)	6896(6)	3.5
S(4)	-4837(4)	644(1)	3715(6)	3.3
C(1)	-433(12)	123(3)	837(19)	2.3
C(2)	-1284(13)	599(3)	4228(19)	2.6
C(3)	-2749(14)	501(3)	2988(20)	2.9
C(1A)	-102(18)	1311(4)	5406(25)	4.1
C(2A)	-132(18)	1654(4)	7214(27)	4.6
C(3A)	582(18)	1989(4)	6130(25)	4.4
C(4A)	473(18)	2339(4)	7934(26)	4.4
C(5A)	1185(19)	2680(4)	6945(28)	5.2
C(6A)	990(20)	3028(4)	8734(29)	5.3
C(7A)	1677(20)	3374(4)	7754(30)	5.6
C(8A)	1479(21)	3721(4)	9571(31)	6.1
C(9A)	2092(23)	4077(4)	8536(35)	7.0
C(10A)	1895(27)	4424(5)	10328(41)	9.0
C(11A)	2437(34)	4768(6)	9354(49)	11.6
C(1B)	-5912(14)	881(3)	677(21)	3.2
C(2B)	-5115(18)	1234(4)	35(25)	4.4
C(3B)	-5202(16)	1561(4)	2004(23)	3.9
C(4B)	-4479(18)	1908(4)	1234(26)	4.7
C(5B)	-4629(18)	2249(4)	3028(26)	5.0
C(6B)	-3946(18)	2599(4)	2074(26)	4.9
C(7B)	-4102(19)	2952(4)	3888(28)	5.4
C(8B)	-3415(20)	3292(4)	2852(30)	5.6
C(9B)	-3605(21)	3651(4)	4603(31)	6.2
C(10B)	-2937(24)	3990(5)	3616(36)	7.5
C(11B)	-3147(28)	4353(6)	5349(44)	9.8

arranged side by side along the a -axis, there exists intercolumnar S...S contact (3.71 Å), nearly the same as that of TTC₈-TTF (Form I) (3.708(8) Å).³⁾

TTC₁₁-TTF: The atomic parameters are listed in Table 5.¹²⁾ The crystal structure is isostructural to the Form I crystals ($n=8, 9, 10$), and all alkyl chains are arranged uniformly. Although the intracolumnar overlapping mode seems to be the same as those of the other Form I crystals ($n=8, 9, 10$), the interplanar distance between the central C₆S₈ skeletons (3.41 Å) and the intracolumnar S...S distance (3.557(5) Å) is shortest in these compounds ($4 \leq n \leq 11$). The shortest intercolumnar S...S distance (3.702(4) Å) is nearly equal to those of the other Form I crystals.

Discussion

The physical properties of TTC _{n} -TTF ($1 \leq n \leq 11$) are shown in Table 6. Two types of molecular conformations of TTC _{n} -TTF are found to exist. In the case of small n ($1 \leq n \leq 3$), the molecular structures are boat-like. On the other hand, the molecules are chair-like, thus making columnar structures over the range of large n ($n \geq 4$). Moreover, these chair-like structures can be divided into the three types (I, II, III) according to differences in the arrangement of their alkyl chains. The angles between the C₆S₈ planes and the alkyl zigzag planes are shown in Fig. 4 ($n \geq 4$). In crystals with $n=4, 5, 6$, though one alkyl chain is nearly perpendicular to the central C₆S₈ groups, the other chain is bent and the zigzag mode is not uniform (Chair III). In crystals with $n \geq 7$, the alkyl chains are far from perpendicular to the central skeleton. In addition, they are divided into two groups (Chair I and Chair II). The alkyl chains of the Chair I type are elongated parallel to each other, while one alkyl chain is slightly bent compared with the other chain in the Chair II structure. These long alkyl

chains result in the characteristic crystal structures. The molecular packings in crystals with $4 \leq n \leq 11$ can be divided into three forms (Form I, II, III). The crystals with the Chair III molecular conformations are included in the Form III group. Compounds with $n=7$ (the triclinic and monoclinic phases), 8, 9 (the monoclinic phase) are Form II, while those with $n=8, 9$ (the triclinic phase), 10, 11 belong to Form I. TTC₈-TTF and TTC₉-TTF can crystallize into the two forms; Form I is the stable phase at room temperature.³⁾ The characteristic difference in the crystal structure between Form I and Form II is the arrangement of the alkyl chains.³⁾ In Form I, all alkyl chains elongate approximately

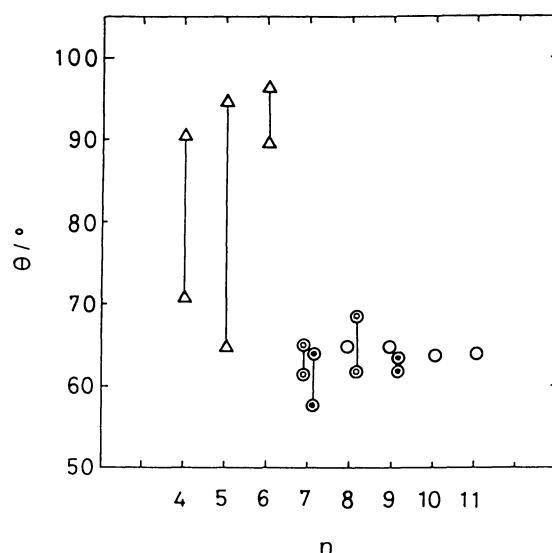
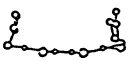
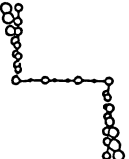
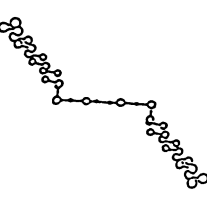


Fig. 4. Angles between the two alkyl chains in the asymmetric unit and the C₆S₈ planes of TTC _{n} -TTFs ($n \geq 4$). Δ : Form III; \odot : Form II (T); \bullet : Form II (M); \circ : Form I.

Table 6. Profiles of TTC _{n} -TTF ($1 \leq n \leq 11$)

	n	Color	Crystal shape	Structure type	Molecular conformation	Space group	d_{calcd} g cm ⁻³	ρ_{RT} Ω cm	E_a eV	T_s °C	$T_m^{(2)}$ °C
	1	¹⁵⁾ Yellow	Plate		Boat	$P 2_1/n$	1.568	2.9×10^{10}	0.38		96.5
	2	⁵⁾ Yellow	Plate		Boat	$P 2_1/c$	1.446	1.2×10^{10}	0.29		70.6
	3	Yellow	Plate		Boat	$P\bar{1}$	1.350	9.6×10^9	0.52		30.4
	4	Orange	Needle	Form III	Chair III	$P\bar{1}$	1.308	6.2×10^6	0.22		24.6
	5	⁵⁾ Orange	Needle	Form III	Chair III	$P\bar{1}$	1.240	6.4×10^7	0.29		32.2
	6	Orange	Needle	Form III	Chair III	$P\bar{1}$	1.195	3.0×10^7	0.28		28.6
	7	Orange	Needle	Form II(T)	Chair II	$P\bar{1}$	1.174	2.5×10^7	0.25		44.0
		Orange	Needle	Form II(M)	Chair II	$P 2_1/a$	1.174	3.8×10^7	0.26		44.0
	8	Orange	Plate	Form I	Chair I	$P\bar{1}$	1.179	1.2×10^5	0.18	33	
		Orange	Needle	Form II(T)	Chair II	$P\bar{1}$	1.147	7.0×10^7	0.21		47.0
	9	Orange	Plate	Form I	Chair I	$P\bar{1}$	1.160	3.5×10^6	0.10	53	
		⁵⁾ Orange	Needle	Form II(M)	Chair II	$P 2_1/a$	1.149	5.0×10^7	0.21		56.8
	10	⁵⁾ Orange	Plate	Form I	Chair I	$P\bar{1}$	1.148	3.7×10^5	0.13	56	59.4
	11	Orange	Plate	Form I	Chair I	$P\bar{1}$	1.137	5.6×10^5	0.17		63.6

parallel to each other and make more dense crystal packing than those in Form II. For $\text{TTC}_7\text{-TTF}$ and $\text{TTC}_9\text{-TTF}$, although the intermolecular interchain packing manner of the triclinic phase is different from that of the monoclinic phase, their molecular structures, stacking manner and physical properties are almost similar. Thus, both phases can be included in the Form II group if we allow for their irregular alkyl chains; they are called Form II (T: triclinic) and Form II (M: monoclinic), respectively. The molecules in the Form I crystals have a greater number of contacts among the sides of the alkyl chains, and the van der Waals interactions could be stronger than that in Form II. The chair-like structure might be favorable for the neighboring alkyl chains to be arranged uniformly. One reason for the inclined alkyl chains could be the narrow width (ca. 3.4 Å) between the outer two S atoms (S(3) and S(4)), which are linked to the alkyl chains, in comparison with the intra- and intermolecular distances between the C atoms of the neighboring alkyl chains (ca. 4.1 Å). The C(1A) atom of one alkyl group is greatly bent, and the alkyl chain including C(1A)—C(8A) is elongated zigzag, thus avoiding repulsion between the H atoms of the neighboring alkyl chains in a molecule. Actually, in short chain compounds ($4 \leq n \leq 6$), although one alkyl chain is elongated upwards, the other chain is slightly bent, and their zigzag mode is not uniform. Moreover, in Form I, since the intermolecular contacts along the b -axis are only with the end of the chains, only a little space exists around the end methyl part (C(9B) for $n=9$) of one alkyl chain (Fig. 2(c)). In Form II, however, the ends of the chains cross each other along

the b -axis (Fig. 2(a) and (b)), thus producing more contacting among the terminal parts of the chains, compared with those in Form I.

The distances between the adjacent least-squares C_6S_8 planes along the stacking axis for the chair-like structures ($4 \leq n \leq 11$) are shown in Fig. 5. The interplanar distances in the Form III crystals are longer than those in the Form II (T and M) and Form I crystals. Especially in Form I crystals, the interplanar distances are significantly shorter than those of the other forms, and gradually decrease with increasing chain length (n). The shortest intracolumnar $\text{S} \cdots \text{S}$ distances in Form I also tend to decrease ($n=8$: 3.5834(9) Å (0°C),²⁾ $n=9$: 3.581(1) Å, $n=10$: 3.569(1) Å,⁵⁾ $n=11$: 3.557(5) Å). In Form II crystals, the shortest $\text{S} \cdots \text{S}$ distances of the triclinic phases ($n=7$: 3.591(2) Å, $n=8$: 3.595(4) Å) are obviously longer than those of Form I. In the case of the monoclinic phases, although only the shortest $\text{S} \cdots \text{S}$ distances ($n=7$: 3.54(1) Å, $n=9$: 3.567(3) Å) are shorter, the molecular overlaps seem to be smaller than those of the Form I crystals (Fig. 3(a), (b), (c)). These structural results mean that the van der Waals attraction forces most efficiently increase, and can depress the volume of the central C_6S_8 moieties in Form I by means of effective contacts among the side alkyl chains in the uniform packing. These results are also associated with the fact²⁾ that the ratio of the effective volumes between the C_6S_8 moiety and four alkyl chains (V_0/V) shows a significant change between $n=7(2.9)$ and $8(4.0)$. The

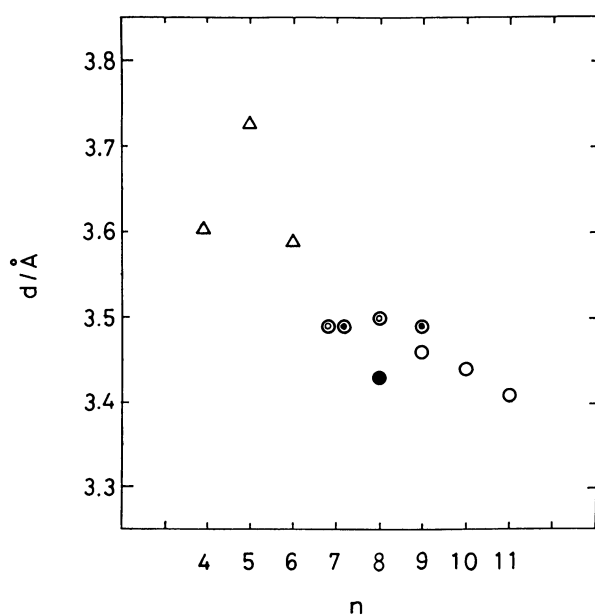


Fig. 5. Distances between the least-squares planes along the c -axis of $\text{TTC}_n\text{-TTFs}$ ($n \geq 4$). Δ : Form III; \odot : Form II (T); \ominus : Form II (M); \circ : Form I. Filled circle of $\text{TTC}_8\text{-TTF}$ means Form I measured at 0°C .

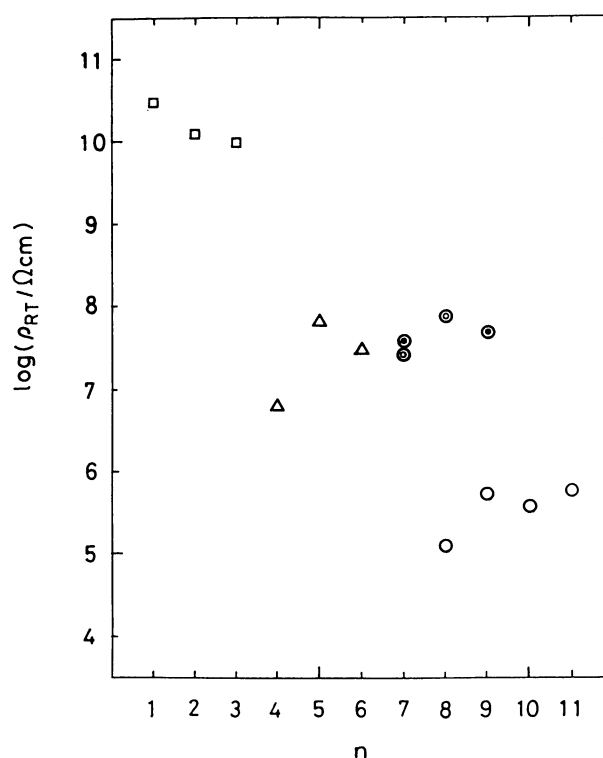


Fig. 6. Electrical resistivities of the $\text{TTC}_n\text{-TTF}$ single crystals ($1 \leq n \leq 11$). \square : Boat form; Δ : Form III; \odot : Form II (T); \ominus : Form II (M); \circ : Form I.

larger densities of the Form I crystals ($n=8, 9$) also indicate their closer packing, compared with Form II.

We shall now discuss the electrical properties, while considering the results of a structure analysis. The electrical resistivities of $\text{TTC}_n\text{-TTF}$ ($1 \leq n \leq 11$) are shown in Fig. 6. The results of a crystal structure analysis imply that the electrical properties drastically change between $n=3$ and 4. The crystals whose molecular structures are boat-like forms ($n=1, 2, 3$) reveal high electrical resistivities (ca. $10^{10} \Omega \text{cm}$), while those with chair-like structures show rather low resistivities (ca. $10^5\text{--}10^7 \Omega \text{cm}$) along the stacking axis. The resistivities in the Form II (T and M) crystals are almost the same as those in the Form III crystals, in spite of their shorter interplanar distances (ca. $10^7 \Omega \text{cm}$). The reason could be their smaller intracolumnar overlap and poor quality of the Form II single crystals compared with the Form III crystals. The resistivities in the Form I crystals (ca. $10^5 \Omega \text{cm}$) are obviously smaller than those of the other forms. The shorter interplanar distances and larger molecular overlaps along the stacking axis in the Form I crystals mean that they have larger transfer integrals compared with those of Form II and Form III. This result is compatible with their lower electrical resistivities (ca. 10^2 times) and activation energies.

In addition, only Form I crystals underwent a phase transition with a steep increase in the electrical resistivity ($n=8$: at 33°C , $n=9$: at 53°C , $n=10$: at 56°C). It was almost impossible to find a phase transition in the resistivity of the $\text{TTC}_{11}\text{-TTF}$ crystal. On the other hand, Form II (both the triclinic ($P\bar{1}$) and monoclinic ($P2_1/a$) phases) and Form III did not exhibit any phase transition up to the melting points. It was found that the solid-solid phase transition for $\text{TTC}_8\text{-TTF}$ is the result of a structural transformation from Form I to Form II with a small movement of the alkyl chains.³⁾ The alkyl chains in Form I somewhat move into the space, thus avoiding thermal collisions between the motions of the chains; simultaneously, the C_6S_8 skeletons may follow the motion of the octyl chains and the change in the intermolecular overlap integrals may cause a change in the electronic band width. The origin of the phase transition for the $\text{TTC}_9\text{-TTF}$ and $\text{TTC}_{10}\text{-TTF}$ crystals should be the same, since they are isostructural with $\text{TTC}_8\text{-TTF}$ (Form I).

In summary, in $\text{TTC}_n\text{-TTF}$ crystals with boat-like structures ($n=1, 2, 3$), the alkyl chains prevent any extension of the overlapping of the central π -electron system. The fairly good conductivities of the $\text{TTC}_n\text{-TTF}$ crystals with long alkyl chains ($n \geq 4$) are caused by the effective overlap between the adjacent central π -systems. The long alkyl chains ($n \geq 4$) can assemble $\text{TTC}_n\text{-TTF}$ molecules in such a fashion that the central

C_6S_8 groups can pile up one after the other very tightly (Molecular Fastener Effect). In Form II and Form III crystals, however, although the intracolumnar interactions through the alkyl chains are effective, the intercolumnar interactions seem to be weak (especially in the Form III crystals, this fact could be one reason for their rather low melting points) since the neighboring alkyl chains are not parallel to each other. In Form I crystals ($n \geq 8$), there exist many effective intra- and intercolumnar contacts among the highly oriented alkyl chains; their van der Waals attractive forces should thus be rather strong and they should efficiently depress the interplanar distances along the stacking axis.

We would like to thank Professor T. Enoki (Tokyo Institute of Technology) for his helpful discussion.

References

- 1) C. Nakano, T. Mori, K. Imaeda, N. Yasuoka, Y. Maruyama, H. Inokuchi, N. Iwasawa, and G. Saito, *Bull. Chem. Soc. Jpn.*, in press.
- 2) Z. Shi, T. Enoki, K. Imaeda, K. Seki, P. Wu, H. Inokuchi, and G. Saito, *J. Phys. Chem.*, **92**, 5044 (1988).
- 3) C. Nakano, K. Imaeda, T. Mori, Y. Maruyama, H. Inokuchi, N. Iwasawa, and G. Saito, *J. Mater. Chem.*, **1**, 37 (1991).
- 4) Y. Li, C. Nakano, K. Imaeda, H. Inokuchi, Y. Maruyama, N. Iwasawa, and G. Saito, *Bull. Chem. Soc. Jpn.*, **63**, 1857 (1990).
- 5) K. Imaeda, T. Enoki, Z. Shi, P. Wu, N. Okada, H. Yamochi, G. Saito, and H. Inokuchi, *Bull. Chem. Soc. Jpn.*, **60**, 3163 (1987).
- 6) P. Wu, G. Saito, K. Imaeda, Z. Shi, T. Mori, T. Enoki, and H. Inokuchi, *Chem. Lett.*, **1986**, 441.
- 7) N. Okada, H. Yamochi, F. Shinozaki, K. Oshima, and G. Saito, *Chem. Lett.*, **1986**, 1861.
- 8) P. Main, S. E. Hull, L. Lessinger, G. Germain, J. P. Declercq, and M. M. Woolfson, *MULTAN82* (1982), Univ. of York, England, Louvain, and Belgium.
- 9) "International Tables for X-Ray Crystallography," Kynoch Press, Birmingham (1974), Vol. IV.
- 10) T. Sakurai and K. Kobayashi, *Rep. Inst. Phys. Chem. Res.*, **55**, 69 (1979).
- 11) Enraf-Nonius (1985), Structure Determination Package. Enraf-Nonius, Delft, The Netherlands.
- 12) Tables of anisotropic thermal parameters, atomic parameters of H-atoms, bond lengths, bond angles, and list of structure factors for both crystals are deposited as Document No. 9014 at the Office of the Editor of *Bull. Chem. Soc. Jpn.*
- 13) H. M. M. Shearer and V. Vand, *Acta Crystallogr.*, **9**, 379 (1956).
- 14) P. W. Teare, *Acta Crystallogr.*, **12**, 294 (1959).
- 15) C. Katayama, M. Honda, H. Kumagai, J. Tanaka, G. Saito, and H. Inokuchi, *Bull. Chem. Soc. Jpn.*, **58**, 2272 (1985).